Indenyl-Nickel Complexes Bearing a Pendant, Hemilabile Olefin Ligand: Preparation, Characterization, and Catalytic Activities

Daniel Gareau, Christine Sui-Seng, Laurent F. Groux, François Brisse, and Davit Zargarian*

Département de Chimie, Université de Montréal, Québec, Canada H3C 3J7

Received April 13, 2005

The reaction of $(PPh_3)_2NiCl_2$ with Li[Ind∧CH=CH_2] gave the neutral complexes (η:η^0-Ind∧CH=CH_2)Ni(PPh_3)Cl (Ind = indenyl; ∧ = $(CH_2)_2$, **1a**; $Si(Me)_2CH_2$, **1b**), which were subjected to Cl^- abstraction to give the corresponding cationic complexes [(η:η^2-Ind∧CH=CH_2)Ni(PPh_3)]$^+$ (∧ = $(CH_2)_2$, **2a**; $Si(Me)_2CH_2$, **2b**). The bis(phosphine) derivatives [(η:η^0-Ind-CH_2CH_2CH=CH_2)Ni($PPh_3)_2$]$^+$ (**3a**) and [(η^3-allyl)Ni($PPh_3)_2$]$^+$ (**4**) formed gradually from room-temperature solutions of **2a** and **2b**, respectively, even in the absence of added PPh_3. On the other hand, [(η:η^0-Ind-$SiMe_2CH_2CH$=CH_2)Ni($PPh_3)_2$]$^+$ (**3b**) was detected only when PPh_3 was added to a CD_2Cl_2 solution of **2b**. The lability of the vinyl moiety in **2** allows these complexes to act as single-component precatalysts for the polymerization and hydrosilylation of styrene; the latter reaction requires little or no induction period with the hydrosilanes $PhRSiH_2$ (R= Ph, Me, H) and proceeds with up to 1000 catalytic turnovers. Compounds **1a**, **1b**, **2a**, **3a**, and **4** have been characterized by NMR and single-crystal X-ray diffraction studies, whereas **2b** and **3b** were identified by NMR spectroscopy. Structural information gleaned from both solid-state and solution data provide important information on the Ni−olefin bonding in **2a** and **2b** and indicate that the Ni−Ind interactions in these complexes are affected by the significant *trans* influence of the chelating olefin moiety.

Introduction

Recent reports have shown that the in-situ-generated cationic indenyl-nickel complexes [IndNi(PPh_3)]$^+$ (Ind = indenyl or its substituted derivatives) can catalyze the dimerization of ethylene,[1] oligo- and polymerization of styrene and norbornene,[2] and hydrosilylation of some olefins and ketones.[3] The catalytic activities of these coordinatively unsaturated, highly electrophilic species depend on the substrate concentration, such that the catalysis proceeds efficiently in the presence of a large excess of substrate but drops off precipitously with decreasing substrate concentration. This loss of activity stems from the tendency of the active species [IndNi(PPh_3)]$^+$ to decompose into an unknown number of side-products, including the much less active bis(phosphine) complexes [IndNi($PPh_3)_2$]$^+$ (Scheme 1).

One strategy for circumventing this inherent deactivation pathway consists of functionalizing the Ind ligand with a tethered, hemilabile moiety L that can occupy the open site around the Ni center to prevent the formation of the bis(phosphine) derivatives. The effectiveness of this strategy is predicated on two factors: (a) the intramolecular L→Ni interaction enables the relatively weakly nucleophilic moieties L to compete effectively with the much more nucleophilic phosphines because of the chelation effect; (b) the reversible nature of the L→Ni interaction allows the substrates, which are usually present in large excess, to approach the Ni center, thereby facilitating the catalysis. Thus, we have shown that the complexes [(η:η^1-Ind∧NR'_2)Ni(PR_3)]$^+$ (∧ = various linkers tethering NR'_2 moieties to Ind) are efficient, single-component catalysts for the polymerization and hydrosilylation of styrene and dimerization of ethylene; as expected, the catalytic activities of these systems are highly dependent on the nucleophilicity of the hemilabile amine moiety (Scheme 2).[4]

Scheme 1

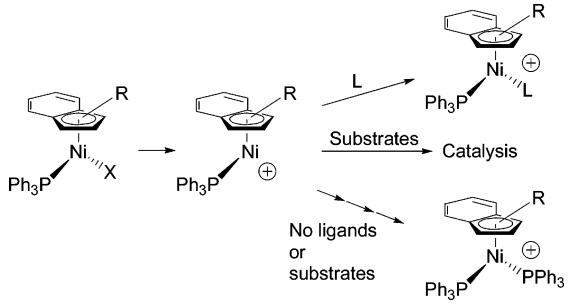

* Corresponding author. Tel: 514-343-2247. Fax: 514-343-2468. E-mail: zargarian.davit@umontreal.ca.

(1) (a) Vollmerhaus, R.; Bélanger-Gariépy, F.; Zargarian, D. *Organometallics* **1997**, *16*, 4762. (b) Dubois, M.-A.; Wang, R.; Zargarian, D.; Tian, J.; Vollmerhaus, R.; Li, Z.; Collins, S. *Organometallics* **2001**, *20*, 663.

(2) (a) Dubois, M.-A. M.Sc. Thesis, Université de Montréal, 2000. (b) Sun, H.-M.; Li, W.-F.; Han, X.; Shen, Q.; Zhang, Y. *J. Organomet. Chem.* **2003**, *688*, 132. (c) Li, W.-F.; Sun, H.-M.; Shen, Q.; Zhang, Y.; Yu, K.-B. *Polyhedron* **2004**, *23*, 1473. (d) Jiménez-Tenorio, M.; Puerta, M. C.; Salcedo, I.; Valerga, P.; Costa, S. I.; Silva, L. C.; Gomes, P. T. *Organometallics* **2004**, *23*, 3139.

(3) Fontaine, F.-G.; Nguyen, R.-V.; Zargarian, D. *Can. J. Chem.* **2003**, *81*, 1299.

10.1021/om050285u CCC: $30.25
Publication on Web 06/28/2005

Scheme 2

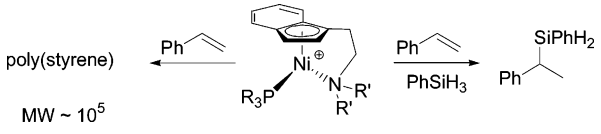

The success of the above approach prompted us to investigate the reactivities of analogous systems bearing hemilabile functional groups other than amines. We elected to study the complexes $[(\eta:\eta^2\text{-Ind}\wedge\text{olefin})\text{Ni}(\text{PR}_3)]^+$ because they resemble a key intermediate in the proposed mechanism for the reactions of olefins with the in-situ-generated $[\text{IndNi}(\text{PR}_3)]^+$; these target complexes would, therefore, provide a rare opportunity to investigate the structural properties and reactivities of species that are closely related to a fleeting intermediate in the above-discussed catalytic reactions.

This report presents the synthesis and characterization of the complexes $(\eta:\eta^0\text{-Ind}\wedge\text{CH}{=}\text{CH}_2)\text{Ni}(\text{PPh}_3)\text{Cl}$ ($\wedge = (\text{CH}_2)_2$, **1a**; $\text{Si}(\text{Me})_2\text{CH}_2$, **1b**) and the corresponding cationic derivatives $[(\eta:\eta^2\text{-Ind}\wedge\text{CH}{=}\text{CH}_2)\text{Ni}(\text{PPh}_3)]^+$ ($\wedge = (\text{CH}_2)_2$, **2a**; $\text{Si}(\text{Me})_2\text{CH}_2$, **2b**) and $[(\eta:\eta^0\text{-Ind}\wedge\text{CH}{=}\text{CH}_2)\text{Ni}(\text{PPh}_3)_2]^+$ ($\wedge = (\text{CH}_2)_2$, **3a**; $\text{Si}(\text{Me})_2\text{CH}_2$, **3b**). The spontaneous formation of the known complex $[(\eta^3\text{-allyl})\text{Ni}(\text{PPh}_3)_2]^+$ (**4**) from **2b** is also described. NMR characterization of compounds **1**−**4**, solid-state structural studies of complexes **1a**, **1b**, **2a**, **3a**, and **4**, and reactivity studies in the polymerization and hydrosilylation of styrene will be described. Complexes **2** represent the first indenyl-nickel complexes containing a π-bound olefin, but the related complexes $(\eta^5:\eta^2\text{-}(\text{C}_5\text{R}_4)(\text{CH}_2)_3\text{CH}{=}\text{CH}_2)\text{NiX}$ (R = H, Me; X = Br, I, Me, Et, *i*-Pr) and $[(\eta^5:\eta^2\text{-}(\text{C}_5\text{Me}_4)(\text{CH}_2)_n\text{CH}{=}\text{CH}_2)\text{Ni}(\text{PPh}_3)]^+$ (n = 2, 3) have been reported previously.[5]

Result and Discussion

Synthesis and Characterization of Complexes 1. The reaction of Li[Ind] with $\text{Cl}\wedge\text{CH}{=}\text{CH}_2$ gave the ligands $\text{H}[\text{Ind}\wedge\text{CH}{=}\text{CH}_2]$,[6] which were deprotonated and reacted with $\text{Ni}(\text{PPh}_3)_2\text{Cl}_2$ to give the complexes $(\eta:\eta^0\text{-Ind}\wedge\text{CH}{=}\text{CH}_2)\text{Ni}(\text{PPh}_3)\text{Cl}$ ($\wedge = (\text{CH}_2)_2$, **1a**; $\text{Si}(\text{Me})_2\text{CH}_2$, **1b**) in 21% (**1a**) and 65% (**1b**) yields (Scheme 3).

Isolation of pure samples of **1a** and **1b** was complicated by the high solubility of these complexes in all common solvents, including hexane. The particularly low yield of **1a** was also caused by the formation, in fairly large quantities, of $(\text{PPh}_3)_3\text{NiCl}$. This Ni(I) byproduct has been encountered previously during the syntheses of other Ind-Ni derivatives, including the parent compound (indenyl)$\text{Ni}(\text{PPh}_3)\text{Cl}$.[7] We have proposed that the side-reaction leading to $(\text{PPh}_3)_3\text{NiCl}$ is initiated by the Ni-promoted coupling of the Ind ligands, which results in the formation of $(\text{PPh}_3)_n\text{Ni}^{(0)}$; the latter then undergoes a comproportionation reaction with the Ni(II) precursor $(\text{PPh}_3)_2\text{NiCl}_2$ to give $(\text{PPh}_3)_3\text{NiCl}$. It is not clear why this side-reaction occurs with $\text{Li}[\text{Ind}\text{-}(\text{CH}_2)_2\text{CH}{=}\text{CH}_2]$ but not $\text{Li}[\text{IndSiMe}_2\text{CH}_2\text{CH}{=}\text{CH}_2]$. The different steric, electronic, and/or chelating properties of these ligands are presumably responsible for the observed differences in their reactivities, but no simple correlation is discernible among the ligands Li[R-Ind] that lead to the formation of $(\text{PPh}_3)_3\text{NiCl}$ (e.g., R= H,[7] $\text{CH}_2\text{CH}_2\text{CH}{=}\text{CH}_2$) and those that do not (e.g., R = Me,[8] $\text{CH}_2\text{CH}_2\text{NMe}_2$,[4a−c] $\text{SiMe}_2\text{CH}_2\text{CH}{=}\text{CH}_2$). It should be emphasized, however, that once isolated, both **1a** and **1b** are stable in solution over a few days.

The ^{1}H, $^{13}\text{C}\{^1\text{H}\}$, and $^{31}\text{P}\{^1\text{H}\}$ NMR spectra of complexes **1a** and **1b** are quite similar to the corresponding spectra of the previously studied derivatives (1-R-Ind)$\text{Ni}(\text{PPh}_3)\text{Cl}$.[9] For instance, each $^{31}\text{P}\{^1\text{H}\}$ NMR spectrum displays a sharp singlet at ca. 30 ppm, while the ^{1}H and $^{13}\text{C}\{^1\text{H}\}$ NMR spectra show the normally observed resonances for this family of complexes, including the characteristically upfield signals for H3 and C3 (see Scheme 3 for the numbering scheme).[10] Furthermore, the sharp $^{13}\text{C}\{^1\text{H}\}$ signals observed for the side-chain carbons imply that the vinyl moiety is not involved in a dynamic process of coordination−dissociation; this contrasts with the observation of a dynamic, temperature-dependent coordination−dissociation process for some of the analogous amino-indenyl derivatives[4a−d] and confirms that the vinyl moiety has a lower nucleophilicity toward nickel.

Comparison of the chemical shifts for some of the ^{13}C signals in these complexes also revealed interesting observations on the electronic effects of the silyl substituent.[11] For instance, the ^{13}C nuclei directly bonded to Si in **1b** (C1 and C9) resonate upfield of the corresponding nuclei in **1a**: 93.6 ppm vs 107.2 ppm, and 24.4 ppm vs 26.9 ppm, respectively. For the three ^{13}C nuclei once removed from Si, the signals for two (C2 and C7a) appear more downfield in **1b** than in **1a** (109.7 ppm vs 103.4 ppm, and 134.4 ppm vs 130.4 ppm, respectively), while the third (C10) shows the opposite trend (135.4 ppm in **1b** vs 139.0 ppm in **1a**).

Single crystals of **1a** and **1b** suitable for X-ray analysis were obtained by slow diffusion of hexane into a saturated Et_2O solution. The crystal data and details of data collection are listed in Table 1, a selection of structural parameters is given in Table 2, and ORTEP drawings are given in Figures 1 and 2. The solid-state structures for **1a** and **1b** are very similar to those of

(4) (a) Groux, L. F.; Bélanger-Gariépy, F.; Zargarian, D.; Vollmerhaus, R. *Organometallics* **2000**, *19*, 1507. (b) Groux, L. F.; Zargarian D. *Organometallics* **2001**, *20*, 3811. (c) Groux, L. F.; Zargarian D. *Organometallics* **2003**, *22*, 3124. (d) Groux, L. F.; Zargarian D. *Organometallics* **2003**, *22*, 4759. (e) Groux, L. F.; Zargarian, D.; Simon, L. C.; Soares, J. B. P. *J. Mol. Catal. A: Chem*. **2003**, *193*, 51.

(5) Lehmkuhl, H.; Näser, J.; Mehler, G.; Keil, T.; Danowski, F.; Benn, R.; Mynott, R.; Schroth, G.; Gabor, B.; Krüger, C.; Betz, P. *Chem. Ber.* **1991**, *124*, 441.

(6) The ligands $\text{H}[\text{Ind}(\text{CH}_2)_2\text{CH}{=}\text{CH}_2]$ and $\text{H}[\text{IndSi}(\text{Me})_2\text{CH}_2\text{CH}{=}\text{CH}_2]$ have also been prepared by slightly different procedures in the following reports: (a) de Armas, J.; Kolis, S. P.; Hoveyda, A. H. *J. Am. Chem. Soc.* **2000**, *122*, 5977. (b) Ready, T. E.; Chien, J. C. W.; Rausch, M. D. *J. Organomet. Chem.* **1999**, *583*, 11. (c) Cano, J.; Gomez-Sal, P.; Heinz, G.; Royo, P. *Inorg. Chim. Acta* **2003**, *345*, 15.

(7) Huber, T. A.; Bélanger-Gariépy, F.; Zargarian, D. *Organometallics* **1995**, *14*, 4997.

(8) Huber, T. A.; Bayrakdarian, M.; Dion, S.; Dubuc, I.; Bélanger-Gariépy, F.; Zargarian, D. *Organometallics* **1997**, *16*, 5811.

(9) Zargarian, D. *Coord. Chem. Rev.* **2002**, *233*−*234*, 157.

(10) We have shown previously (ref 9) that the upfield shifts of the C3 and H3 nuclei result from the nearly sp^3-hybridization of C3 and the ring currents of PPh_3 phenyl groups.

(11) For an in-depth discussion of the electronic effects of silyl substituents on Cp-type ligands see the following reports: (a) Zachmanoglou, C. E.; Docrat, A.; Bridgewater, B. M.; Parkin, G.; Brandow, C. G.; Bercaw, J. E.; Jardine, C. N.; Lyall, M.; Green, J. C.; Keister, J. B. *J. Am. Chem. Soc.* **2002**, *124*, 9525. (b) Langmaier, J.; Samec, Z.; Varga, V.; Horacek, M.; Choukroun, R.; Mach, K. *J. Organomet. Chem.* **1999**, *584*, 323.

Scheme 3

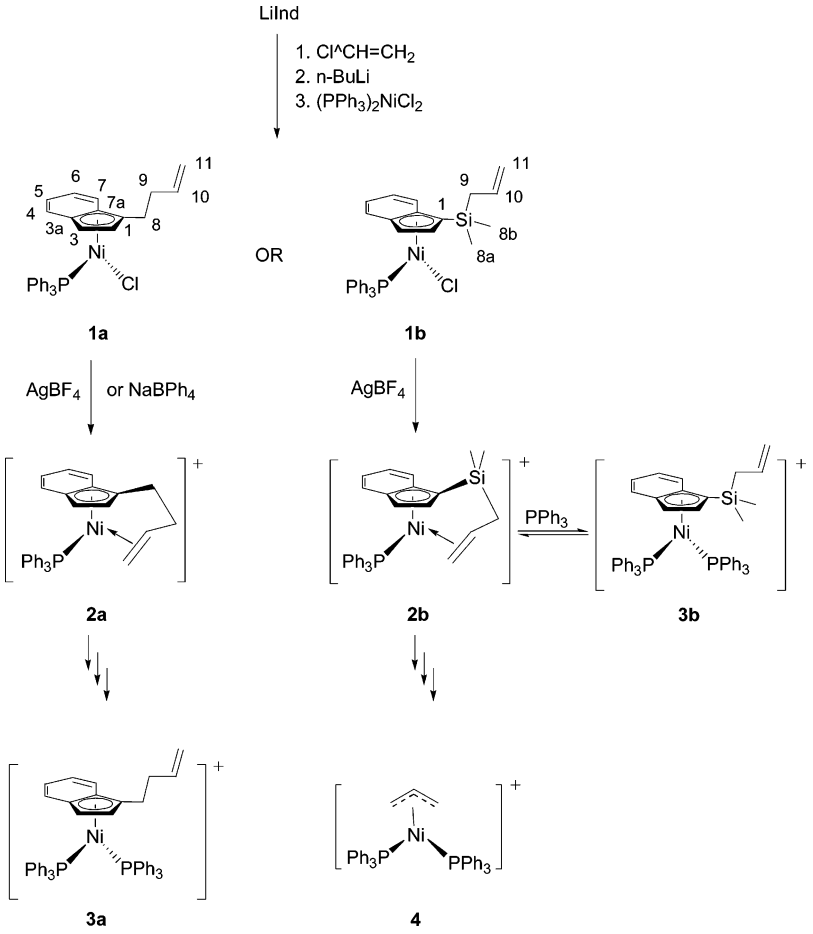

Table 1. Crystal Data, Data Collection, and Structure Refinement Parameters of 1a, 1b, 2a, 3a, and 4

	1a	1b	2a	3a	4
formula	$C_{31}H_{28}ClPNi$	$C_{32}H_{32}ClPSiNi$	$C_{55}H_{48}BPNi$	$C_{73}H_{63}BNiP_2$	$C_{39}H_{35}BF_4NiP_2$
mol wt	525.66	569.80	809.42	1071.69	711.1407
cryst color, habit	red, block	red, block	red, block	yellow, block	yellow, block
cryst dimens, mm	0.16 × 0.30 × 0.30	0.06 × 0.21 × 0.56	0.16 × 0.16 × 0.19	0.50 × 0.43 × 0.08	0.55 × 0.08 × 0.05
symmetry	triclinic	monoclinic	monoclinic	monoclinic	monoclinic
space group	$P\bar{1}$	$C2/c$	$P2_1/n$	$P2_1/n$	$C2/c$
a, Å	9.15590(10)	28.763(9)	15.9152(2)	10.3056(7)	25.0077(3)
b, Å	10.4614(2)	10.667(10)	32.7827(3)	16.2965(11)	17.1191(2)
c, Å	15.5498(2)	19.103(11)	16.5352(2)	33.568(2)	17.6639(2)
α, deg	90.5120(10)	90	90	90	90
β, deg	106.2650(10)	97.44(3)	104.5180(10)	96.119(5)	118.0880(10)
γ, deg	113.8330(10)	90	90	90	90
Z	2	8	8	4	8
D(calcd), g cm^{-1}	1.348	1.302	1.287	1.270	1.416
diffractometer	Bruker AXS SMART 2K	Nonius CAD-4	Bruker AXS SMART 2K	Bruker AXS SMART 2K	Bruker AXS SMART 2K
temp, K	223(2)	223(2)	223(2)	100(2)	100(2)
λ (Kα), Å	1.54178 (Cu)	0.71073 (Mo)	1.54178 (Cu)	1.54178 (Cu)	1.54178 (Cu)
μ, mm^{-1}	2.731	0.875	1.308	1.368	2.168
scan type	ω scan	ω scan	ω scan	ω scan	ω scan
F(000)	548	2384	3408	2256	2944
θ_{max} (deg)	72.91	25.98	72.98	73.20	72.90
h,k,l range	$-11 \le h \le 11$ $-12 \le k \le 12$ $-19 \le l \le 19$	$0 \le h \le 35$ $0 \le k \le 13$ $-23 \le l \le 23$	$-19 \le h \le 19$ $-40 \le k \le 40$ $-20 \le l \le 20$	$-12 \le h \le 12$ $-20 \le k \le 20$ $-36 \le l \le 40$	$-30 \le h \le 30$ $-20 \le k \le 21$ $-21 \le l \le 20$
reflns used ($I > 2\sigma(I)$)	15 611	5684	16 463	10 703	6557
absorption correction	multiscan SADABS	integration Absorption	multiscan SADABS	multiscan SADABS	multiscan SADABS
T (min, max)	0.4100, 0.7300	0.8400, 0.9500	0.6900, 0.8600	0.0400, 0.9300	0.6000, 0.8800
R [$F^2 > 2\sigma(F^2)$], $wR(F^2)$	0.0388, 0.1072	0.0460, 0.1252	0.0434, 0.1126	0.0787, 0.1966	0.0511, 0.1465
GOF	1.12	0.802	0.958	0.999	1.074

the previously studied, closely analogous (1-R-Ind)Ni(PPh$_3$)Cl complexes.[9] The geometry of the Ni center in these complexes can be described as distorted square planar, the largest distortion arising from the small bite angle of the Ind ligand (ca. 65°). The significantly longer Ni−C3a and Ni−C7a distances relative to the Ni−

Table 2. Selected Bond, Distances (Å) and Angles (deg) for 1a, 1b, 2a, and 3a

	1a	1b	2a	3a
Ni−P1	2.1727(5)	2.172(2)	2.2276(6)	2.1956(10)
Ni−Cl or P2	2.1835(6)	2.192(3)		2.2136(11)
Ni−C1	2.1302(19)	2.113(7)	2.0726(19)	2.143(3)
Ni−C2	2.075(2)	2.044(7)	2.069(2)	2.089(3)
Ni−C3	2.034(2)	2.041(7)	2.073(2)	2.052(4)
Ni−C3a	2.292(2)	2.332(7)	2.297(2)	2.299(3)
Ni−C7a	2.332(2)	2.349(7)	2.330(2)	2.364(3)
Ni−C10			2.130(2)	
Ni−C11			2.072(2)	
C1−C2	1.417(3)	1.407(10)	1.427(3)	1.413(5)
C2−C3	1.421(3)	1.393(9)	1.392(3)	1.409(5)
C3−C3a	1.452(3)	1.457(10)	1.465(3)	1.462(5)
C7a−C1	1.461(3)	1.469(10)	1.448(3)	1.482(5)
C10−C11	1.294(6)	1.304(10)	1.356(3)	1.298(7)
P1−Ni−Cl or P2	97.94(2)	96.31(9)		102.42(4)
C3−Ni−Cl or P2	162.42(7)	163.9(2)		162.24(10)
C3−Ni−P1	99.51(7)	99.6(2)	101.96(6)	94.12(11)
C1−Ni−Cl or P2	95.59(6)	97.4(2)		97.55(10)
C1−Ni−P1	166.10(6)	166.2(2)	165.26(6)	159.96(11)
C1−Ni−C3	66.87(9)	66.7(3)	66.80(8)	66.27(14)
ΔM−C[a] (Å)	0.23	0.26	0.24	0.234
HA[b] (deg)	10.35	10.68	11.15	10.76
FA[c] (deg)	9.94	8.74	11.99	12.14

[a] $\Delta(M-C) = 0.5\{(M-C3a + M-C7a)\} - 0.5\{(M-C1 + M-C3)\}$. [b] HA is the angle between the planes formed by the atoms C1, C2, C3 and C1, C3, C3a, C7a. [c] FA is the angle between the planes formed by the atoms C1, C2, C3 and C3a, C4, C5, C6, C7 and C7a.

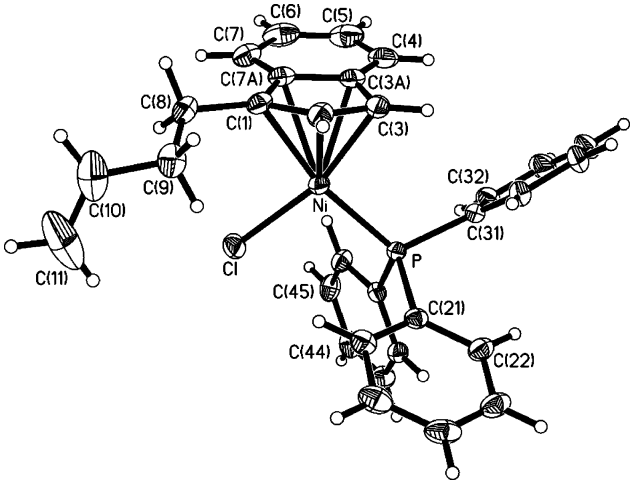

Figure 1. ORTEP view of complex **1a**. Thermal ellipsoids are shown at 30% probability.

C(allyl) bond lengths are in accord with the anticipated lower hapticity of the Ind ligand, the so-called $\eta^5 \rightarrow \eta^3$ slippage, when it is coordinated to relatively electron-rich metal centers. The calculated values of ΔM−C, the slip factor, are in the usual range for the neutral Ni−Cl derivatives (ca. 0.23−0.26 Å); similarly, the significant asymmetry in the Ni−C(allyl) bond lengths (Ni−C1 > Ni−C2 > Ni−C3) reflects the unequal *trans* influences of the PPh_3 and Cl ligands.[9] The pendant olefin moiety is oriented away from the Ni center in both structures.

Synthesis and Characterization of Complexes 2 and 3. Abstraction of Cl^- from **1a** proceeded in the presence of either $NaBPh_4$ or $AgBF_4$ in solvents such as CH_2Cl_2 or C_6H_6 to give the cationic complex **2a** in ca. 50% yield, whereas the analogous conversion of **1b** into **2b** required $AgBF_4$ and proceeded in CH_2Cl_2 only (Scheme 3). The lower solubility of cationic complexes

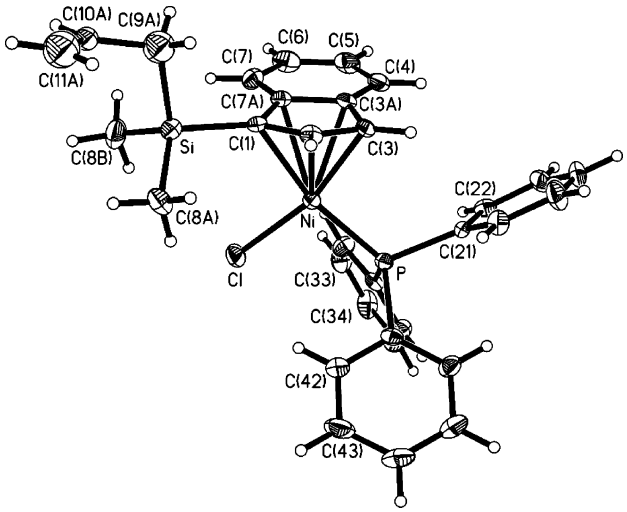

Figure 2. ORTEP view of complex **1b**. Thermal ellipsoids are shown at 30% probability.

2 allowed us to recover ca. 45−50% crude yields, but isolation of pure samples by recrystallization of the crude material was complicated because these compounds undergo a slow decomposition process, as follows.

Monitoring freshly prepared samples of **2a** by $^{31}P\{^1H\}$ NMR spectroscopy showed only one singlet resonance at ca. 34 ppm, but a minor set of AB doublets ($^2J_{P-P}$ = 27 Hz) emerged over a few hours at ca. 35 and 32 ppm. Previous studies had shown that such AB signals correspond to bisphosphine complexes of the type $[(R\text{-Ind})Ni(PPh_3)_2]^+$;[1a,12] we suspected, therefore, that the new species arising from **2a** was the bis(phosphine) side-product $[\eta,\eta^0\text{-IndCH}_2\text{CH}_2\text{CH=CH}_2)Ni(PPh_3)_2]^+$, **3a**. This was confirmed when we observed that adding excess PPh_3 to the sample of **2a** accelerated the growth of the aforementioned AB signals. Given the facile conversion of **2a** to **3a**, isolation of pure samples of **2a** required that the abstraction of Cl^- from **1a** be carried out rapidly (over minutes) and in highly dilute mixtures; this approach furnished single crystals of both **2a** and **3a** suitable for X-ray analyses of these complexes (vide infra).

Complex **2b** was less susceptible to decomposition, but solutions aged over 1 day or longer showed a number of new $^{31}P\{^1H\}$ resonances; interestingly, however, the AB doublets expected for the analogous bis(phosphine) side-product $[\eta,\eta^0\text{-(IndSiMe}_2\text{CH}_2\text{CH=CH}_2)\text{-}Ni(PPh_3)_2]^+$, **3b**, were not detected in these spectra. The absence of **3b** among the species arising from the decomposition of **2b** was intriguing and prompted us to test whether excess PPh_3 would facilitate the formation of **3b**. These tests showed that adding 1 equiv of PPh_3 to a CD_2Cl_2 solution of **2b** resulted in the replacement of the original $^{31}P\{^1H\}$ signal at ca. 33.7 ppm by a broad signal at ca. 31 ppm; this signal collapsed at 188 K into AB doublets at 33.1 and 29.0 ppm ($^2J_{P-P} \approx 32$ Hz). Comparison of these signals to those obtained for **3a** convinced us that they were due to **3b**, which appears to be in equilibrium with **2b**.

The ^1H NMR spectrum was also consistent with the above scenario. For instance, the addition of PPh_3

(12) Fontaine, F.-G. Ph.D. Thesis, Université de Montréal, 2002.

diminished the intensity of the signals due to the chelating vinyl moiety and resulted in the emergence of signals at lower fields (ca. 5−6 ppm), assigned to the nonchelating vinyl moiety. Similarly, the intensity of the signals assigned to the chemically inequivalent $Si(CH_3)_2$ groups in **2b** diminished while a pair of new signals appeared ca. 0.8 ppm upfield of the original signals, presumably because of the interaction of the $SiMe_2$ protons with the PPh_3 ligand; integration of the two sets of $SiMe_2$ signals indicated a 7:1 ratio (at room temperature) in favor of the new species. These observations imply that **2b** can be converted to **3b** in the presence of PPh_3, but this process is reversible because steric repulsion between the $SiMe_2$ group and the adjacent PPh_3 ligand in **3b** allows the olefin moiety to compete effectively for coordination to Ni (Scheme 3).

The C_s symmetry of complexes **2a** and **2b** renders all their nuclei chemically inequivalent, which complicated the ^1H and $^{13}C\{^1H\}$ NMR spectra of these complexes, but signal assignment was facilitated by the COSY and HMQC spectra. Comparing the spectral features of **2** to those of their precursors **1** revealed a number of interesting shifts in many of the signals, indicating important structural differences between these complexes. For instance, significant downfield shifts were noted for H2/H3 (ca. 0.7−2 ppm) and for C1/C2/C3 (ca. 10−20 ppm). These shifts can be attributed to the enhanced hapticity of Ind, which results from the increased electrophilicity of the Ni center in cationic **2**. The downfield shifts noted for H3 also serve as an indirect measure of the *trans* influence of the vinyl moiety, and comparison to previously studied systems allows us to attribute a very strong *trans* influence to olefins, similar to that of CO.[13]

The chelation of the vinyl moiety in **2** was also corroborated on the basis of spectral comparisons, as follows. The primary indicators of the chelation were the upfield shifts of the signals for the vinyl protons H10 (by ca. 0.5 ppm) and H11A/H11B (by ca. 1−2 ppm), as well as the signals for C10 (by ca. 24 ppm) and C11 (by ca. 40 ppm). These shifts can be justified by noting that coordination of the vinyl moiety to Ni increases the sp^3 character of C10 and C11 and places H11A and H11B within the anisotropy cone of the PPh_3 phenyl groups.[14] On the other hand, chelation reduces the flexibility of the side-chain, thereby magnifying the differences in the chemical environments of the CH_2 and $Si(CH_3)_2$ nuclei and increasing the separation of their NMR signals. For instance, the chemical shifts of the $Si(CH_3)_2$ signals are less different in **1b** (0.81 and 0.83 ppm) than in **2b** (0.70 and 0.60 ppm).

(13) We have shown (ref 9) that the chemical shift of the H3 signal in the analogous complexes (1-R-Ind)Ni(PPh_3)X and [(1-R-Ind)Ni(PPh_3)L]$^+$ reflects the Ni−C3 bond strength and hence the *trans* influence of the ligands X and L. The following *trans* influence order has emerged for the ligands studied: Cl (3.30 ppm) < CC−Ph (3.9 ppm) < phthalimidate (4.10 ppm) < Me (4.20 ppm) ∼ pyridine (4.21 ppm) < PR_3 (ca. 4.3−5.1 ppm) < Bu^tNC: (4.80 ppm) < olefin (ca. 5.5 ppm) ∼ CO (5.53 ppm).

(14) The distances measured from the center of the phenyl ring nearest the chelating vinyl moiety (i.e., ring C121−C126 in **2a**) to the vinyl hydrogen atoms are as follows: 5.356 Å for H10; 4.219 Å for H11A.; 3.427 Å for H11B. In their report on the solid-state structure of the related complex (η^5:η^2-(C_5Me_4)(CH_2)$_3$CH=CH_2)NiBr (ref 5), Lehmkuhl et al. have proposed an agostic interaction between Ni and one of the vinylic protons (2.33(8) Å). Although comparable values were noted for the corresponding Ni−H distances in **2a** (2.44 Å for H111A, 2.54 Å for H111B, and 2.52 Å for H110), we are not convinced these distances reflect significant Ni−H interactions.

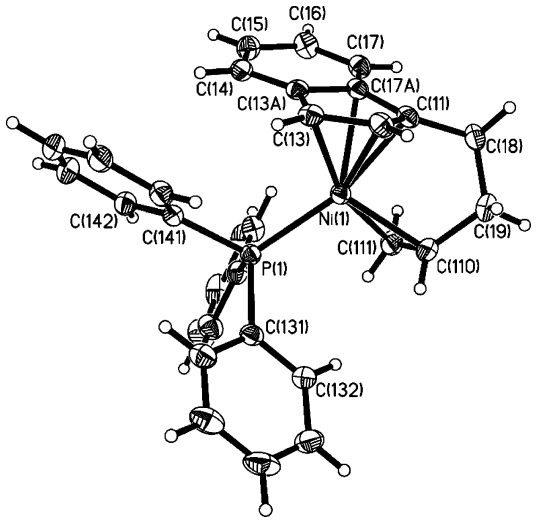

Figure 3. ORTEP view of one of the two independent molecules found in the unit cell of complex **2a**. Thermal ellipsoids are shown at 30% probability.

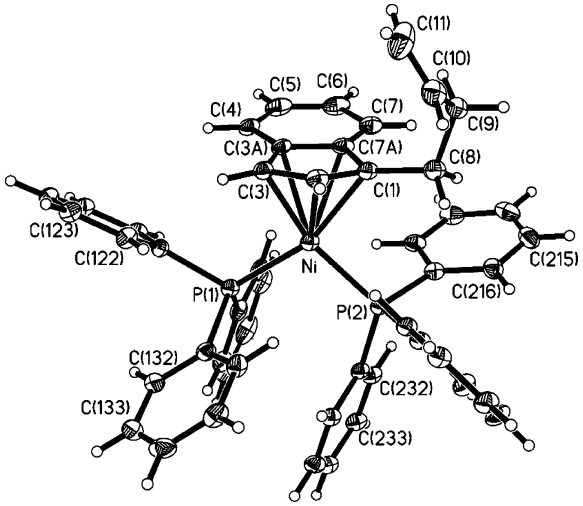

Figure 4. ORTEP view of complex **3a**. Thermal ellipsoids are shown at 30% probability.

As discussed above, the coordination of two PPh_3 ligands in **3** is most clearly evident from the AB doublets in the ^{31}P NMR spectra. The similar chemical shifts for the ^1H signals due to the vinylic protons H11 in **1** and **3** (ca. 5 ppm vs ca. 3−4 ppm for the corresponding signals in **2**) indicate that the olefin moiety in **3** is dangling. On the other hand, the ^1H and ^{13}C signals for Ind nuclei are fairly similar for the cationic complexes **2** and **3**.

Single crystals suitable for X-ray diffraction studies were obtained by repeated recrystallization in CH_2Cl_2/Et_2O for **2a** and CH_2Cl_2/hexane for **3a**. All attempts at growing crystalline samples of **2b** failed, giving instead small quantities of a crystalline species identified as the well-known complex [(η^3-allyl)Ni(PPh_3)$_2$]$^+$, **4** (vide infra). The crystal data and details of data collection for **2a** and **3a** are listed in Table 1, a selection of structural parameters are listed in Table 2, and ORTEP drawings are given in Figures 3 and 4. The solid-state structures of **2a** and **3a** are described below.

The main structural features of the cationic complexes **2a** and **3a** are quite similar to those of the neutral complexes **1**, implying that the displacement of Cl by

Chart 1

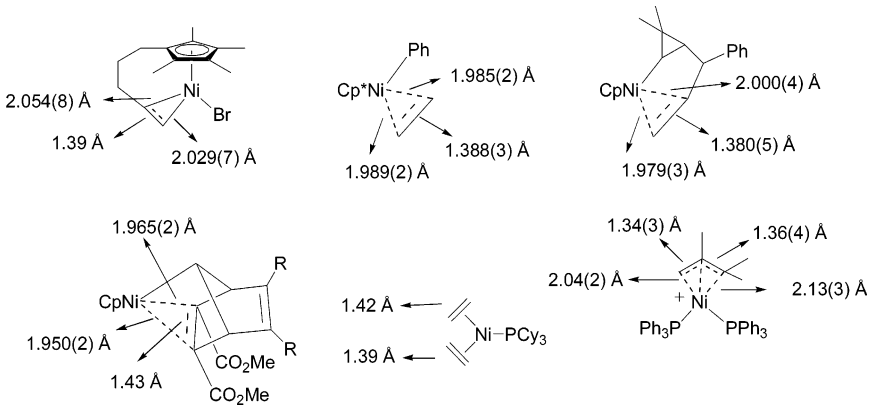

the pendant olefin moiety or a second PPh_3 does not result in major changes in the overall geometry of these complexes. Interestingly, the ΔM−C values for **1a**, **2a**, and **3a** are virtually unchanged, implying no major changes in the Ind−Ni interaction on going from the neutral precursors to cationic derivatives. This contrasts with the stronger Ind−Ni interaction inferred from the solution NMR spectra of **2a** and **3a** (vide supra) and expected on the basis of the presumed increase in the electrophilicity of the Ni center in these cationic species. Similarly, the observation that the Ni−P bonds are longer by about 15−25 esd in cationic **2a** and **3a** relative to neutral **1a** and **1b** might appear counterintuitive at first since the more electrophilic Ni centers appear to be forming weaker Ni−P bonds; this phenomenon can be explained, however, in terms of the lower compatibility between the positively charged, harder Lewis acid Ni center and the soft Lewis base PPh_3.[15]

Despite the overall similarities in the structures of the neutral Ni−Cl precursors **1** and their cationic derivatives **2a** and **3a**, there are important differences in the coordination symmetry of the Ind ligand and the disposition of the tethered olefin moiety in these complexes. Thus, we observe highly symmetrical Ni−C interactions for the allylic carbons in **2a** (Ni−C1 ∼ Ni−C3), implying that the vinyl moiety and PPh_3 have comparable *trans* influences. In contrast, the Ni−C(allyl) interaction is as unsymmetrical in **3a** as it is in **1a** (Ni−C3 < Ni−C1 by ca. 30 esd), even though both of the allylic carbons in **3a** are *trans* from a PPh_3. We attribute the unequal Ni−C1/C3 distances in **3a** to the unequal Ni−P bond lengths (Ni−P2 > Ni−P1 by ca. 18 esd), which are caused by the steric repulsion between the Ind substituent and the PPh_3 adjacent to it; in effect, the two PPh_3 ligands lead to unequal *trans* influences. It is instructive to note that the Ni−C(Cp) interactions in (η^5,η^2-$C_5Me_4(CH_2)_3CH{=}CH_2$)Ni−Br[5] are also unsymmetrical because of the unequal *trans* influences of Br and the chelating vinyl moiety. Moreover, the average Ni−C(Cp) distance in the latter complex is intermediate between the shorter Ni−C1/C2/C3 and the longer Ni−C3a/C7a distances in **2a**; as a result, the allyl-ene distortion is much more evident in **2a**.

The η^2-bound pendant olefin moiety is perhaps the most important feature of the solid-state structure in **2a**. The C−C distance in this moiety is much longer than that in the nonchelating complexes **1** (C10−C11= 1.294(6) Å in **1a** and 1.304(10) Å in **1b** vs 1.356(3) Å in **2a**) but shorter than the corresponding C−C distance in (η^5,η^2-$C_5Me_4(CH_2)_3CH{=}CH_2$)Ni−Br (1.39(1) Å).[5] Similarly elongated C−C bonds (ca. 1.38−1.39 Å) have been observed in the related, charge-neutral Cp−Ni(II) complexes Cp*Ni(Ph)($CH_2{=}CH_2$)[16] and CpNi(R)($CH_2{=}CH_2$)[17] (Chart 1), whereas much greater elongation is observed in an analogous Ni(II) complex bearing electron-withdrawing CO_2Me groups on the olefin moiety (1.43 Å)[18] and in one of the two ethylene moieties in the Ni(0) complex ($CH_2{=}CH_2$)$_2$Ni(PCy_3) (1.42 Å).[19] The elongation of the C−C bond in the Ni-olefin moiety can be attributed to the σ-donation from the olefinic π-electron density into empty Ni orbitals as well as π-back-bonding from the filled Ni d_π orbitals into the empty π^* orbitals of the olefin moiety; the greater elongation found in the charge-neutral Cp complexes is presumably a reflection of more extensive π-back-donation from the more electron-rich, neutral Ni center.

Chart 2

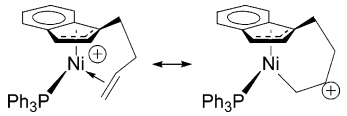

Finally, it is noteworthy that the Ni−C11 distance in **2a** is significantly shorter than Ni−C10 (by ca. 0.06 Å, about 30 times esd), which indicates that the vinyl moiety coordinates to the Ni center in an unsymmetrical fashion; in comparison, the difference in the corresponding Ni−C bonds in (η^5,η^2-$C_5Me_4(CH_2)_3CH{=}CH_2$)Ni−Br[5] is less significant (ca. 0.025 Å, about 3 times esd). It is tempting to propose that this nonsymmetrical interaction implies that a charge-separated canonical form makes significant contributions to the bonding scheme in **2** (Chart 2); this proposal would help explain why olefins susceptible to cationic polymerization (e.g., styrene) are polymerized by this class of Ni cations (vide infra).

Complex 4. As mentioned above, small amounts of **4** were obtained during the attempted recrystallization

(15) For a discussion of Ni−phosphine and Ni−Cp bonding in the complexes Cp*Ni(PR_3)X see: Holland, P. L.; Andersen, R. A.; Bergman, R. G.; Huang, J.; Nolan, S. *J. Am. Chem. Soc.* **1997**, *119*, 12800.

(16) Lehmkuhl, H.; Keil, T.; Benn, R.; Rufinska, A.; Krüger, C.; Poplawska, J.; Bellenbaum, M. *Chem. Ber.* **1988**, *121*, 1931.

(17) Lehmkuhl, H.; Naydowski, C.; Benn, R.; Rufinska, A.; Schroth, G.; Mynott, R.; Krüger, C. *Chem. Ber.* **1983**, *116*, 2447.

(18) Battiste, M. A.; Griggs, B. G., Jr.; Sackett, D.; Coxon, J. M.; Steel, P. J. *J. Organomet. Chem.* **1987**, *330*, 437.

(19) Krüger, C.; Tsang, Y.-H. *J. Organomet. Chem.* **1972**, *34*, 387.

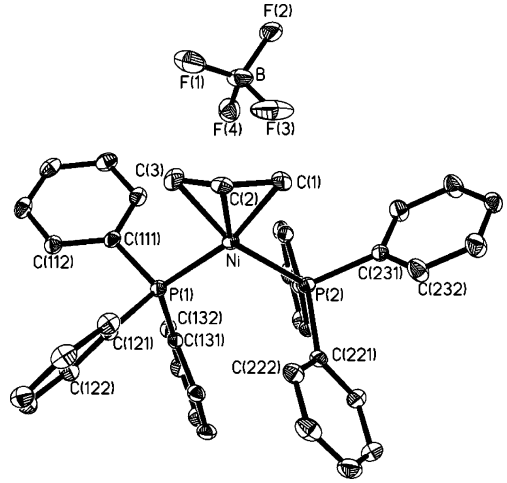

Figure 5. ORTEP view of the major model (60%) for complex **4**. Thermal ellipsoids are shown at 30% probability. Selected bond lengths (Å) and angles (deg): Ni−P1 = 2.2049(8), Ni−P2 = 2.1920(8), Ni−C1 = 2.042(18), Ni−C2 = 2.015(4), Ni−C3 = 2.03(2), C1−C2 = 1.405(13), C2−C3 = 1.320(15), C1−Ni−C3 = 71.4(5), P1−Ni−P2 = 103.12(3).

of **2b**. The NMR spectra of **4** matched those reported previously.[20] The way in which the unexpected but interesting transformation of **2b** to **4** comes about is not known. To be sure, desilylation of SiR_3-substituted indenyl ligands is precedented, but in most previous cases it is the silyl substituent that is eliminated, leaving behind an unsubstituted Ind ligand,[21] whereas in the present case it is the $IndSiMe_2$ fragment that is eliminated, leaving behind the allyl moiety. Since the solid-state structure of this complex had not been reported previously, we undertook an X-ray diffraction study of the crystals obtained, as described below.

The solid-state structure of complex **4** is similar to that of **3a** in that two PPh_3 ligands and the allyl moiety are arranged around the Ni center. The central carbon atom of the allyl moiety (C2) is distorted over two positions, but the disorder was modeled in a satisfactory fashion with two solutions (60:40). The ORTEP diagram and a selection of bond distances and angles for the major model are shown in Figure 5. The geometry around the central Ni(II) is distorted square planar, with a C1−Ni−C3 angle of ca. 71° and a P1−Ni−P2 angle of ca. 103°. The square plane defined by P1, P2, C1, and C3 atoms makes an angle of ca. 115° with the allyl moiety. The Ni−C1/C3 bond lengths are virtually symmetrical, whereas the differences between Ni−P and allylic C−C distances (C1−C2 vs C2−C3) are small but significant. Fairly similar structural parameters are found in the only other structurally characterized Ni-(simple allyl) complex $[(1,1,2\text{-trimethylallyl})Ni(PPh_3)_2]^+$[22] (Chart 1).

Catalytic Polymerization of Styrene. Previous reports have shown that combining $IndNi(PPh_3)Cl$ and $NaBPh_4$ produces an active catalyst that polymerizes styrene at 80 °C over 24−48 h to a mixture of oligo- and poly(styrene).[2] As anticipated, we found that styrene can be polymerized by complex **2b** alone (eq 1, Table 3).[23]

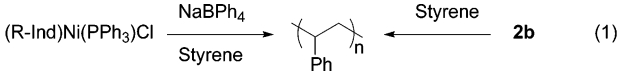

(1)

Optimization experiments demonstrated that the choice of solvent was crucial for the efficacy of the polymerization reactions: using chlorinated solvents such as dichloroethane resulted in small catalytic turnover numbers (ca. 40−60), whereas reactions carried out in nonchlorinated solvents such as toluene or no solvent at all gave ca. 500 turnovers. The GPC analyses of the polymers obtained from the latter experiments showed a bimodal distribution of low molecular weight oligomers ($M_w \sim 1200-1600$) and much higher molecular weight polymers ($M_w \approx (5-7) \times 10^5$); the polydispersities of both fractions were fairly narrow ($M_w/M_n \approx 1.2-1.4$). These results are qualitatively similar to those obtained from the polymerizations catalyzed by $[(\eta,\eta^1\text{-Ind-}CH_2CH_2NMe_2)Ni(PPh_3)]^+$ or the $IndNi(PPh_3)Cl/NaBPh_4$ combination. On the other hand, the polymerizations catalyzed by **2b** appear to be somewhat more facile, as they proceed at milder temperatures (60 °C vs 80 °C); indeed, the reactions catalyzed by **2b** can proceed even at room temperature, albeit with lower catalytic turnover numbers (runs 4 and 5 vs runs 2 and 3).

The polymerization reactions described above can, in principle, proceed via either a Ni-initiated electrophilic route or a Ni-based insertion mechanism. We used NMR spectroscopy in an attempt to shed some light on the reaction pathway; unfortunately, however, the spectra recorded for C_6D_6 solutions (ca. 2 M in styrene and 0.02 M in **2b**, at 60 °C) were uninformative: the ^1H NMR spectra showed only very broad, featureless signals (at ca. 1−4 ppm), whereas the $^{31}P\{^1H\}$ NMR spectra showed no signals at all. Thus, we have been unable to determine which pathway is operative. It seems reasonable, however, to suppose that the first step in the polymerization process is the associative displacement of the chelating vinyl moiety by styrene, giving $[(\eta,\eta^0\text{-Ind-}SiMe_2CH_2CH_2{=}CH)Ni(PPh_3)(\text{styrene})]^+$ (Scheme 4). The nature of the Ni−styrene interaction in this intermediate would have a determining effect on the polymerization mechanism. If we suppose a (partial) positive charge on its α-carbon atom, it follows that the coordinated styrene can undergo a nucleophilic attack by a second molecule of monomer, as shown in Scheme 4; subsequent attacks by styrene would then lead to chain growth.

The above-proposed propagation sequence would then continue until the $Ni-CH_2CH(Ph)-P$ moiety (P = the growing polymer chain) undergoes a β-H elimination to give a Ni−H species and a carbocation-terminated polymer chain. The latter would continue growing via the electrophilic mechanism, with the carbocation acting as the electrophile and the monomer as the nucelophile, to give the high M_w poly(styrene) obtained in our experiments.[24] On the other hand, the Ni−H intermedi-

(20) Castro, B.; Neibecker, D. *J. Organomet. Chem.* **1975**, *85*, C-39.
(21) Wang, B.; Zhu, B.; Xu, S.; Zhou, X. *Organometallics* **2003**, *22*, 4842.
(22) Zocchi, M.; Albinati, A. *J. Organomet. Chem.* **1974**, *77*, C40.
(23) Complex **2a** was not included in the reactivity studies, because its solutions were often contaminated by small amounts of $[(1\text{-}CH_2\text{-}CH_2CH{=}CH_2{-}Ind)Ni(PPh_3)_2]^+$, **3a**, which is inactive in the polymerization reactions but active in the hydrosilylations.
(24) The proposed sequence of electrophilic attacks might also be intramolecular, leading to the formation of cyclic oligomers.

Table 3. Oligo- and Polymerization of Styrene Catalyzed by 2b[a]

run	T (°C)	solvent (mL)	catalytic turnovers	oligomer M_w ($\times 10^3$), M_w/M_n	polymer M_w ($\times 10^4$), M_w/M_n	oligomer:polymer ratio
1[b]	60	$(ClCH_2)_2$ (8)	50		7.9, 2.55	
2	60	toluene (1)	560	1.4, 1.25	61.7, 1.41	90:10
3	60	none	560	1.6, 1.39	58.5, 1.40	85:15
4	25	toluene (1)	50	1.4, 1.20	64.1, 1.35	80:20
5	25	none	120	1.2, 1.27	62.2, 1.42	65:35

[a] Unless otherwise noted, the polymerizations were run over 4 h using a catalyst:monomer ratio of 1:1000. [b] A 1:2000 ratio of **2b**:styrene was used in this run; reaction time = 48 h.

Scheme 4

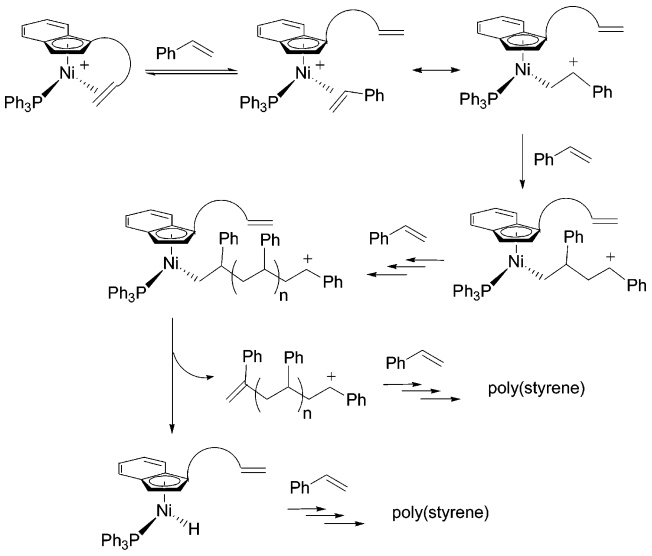

Scheme 5

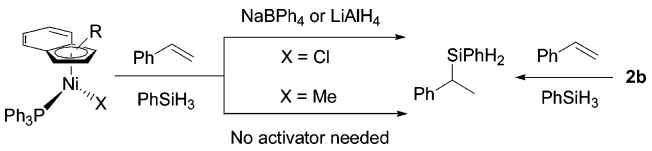

ate could then initiate a different propagation sequence via an insertion mechanism and terminating via a β-hydride elimination pathway.[25]

Catalytic Hydrosilylation Reactions. Previous studies in our group have shown that the IndNi(PPh_3)Cl/$NaBPh_4$ combination can also catalyze the addition of $PhRSiH_2$ (R = Ph, Me, H) to olefins. For instance, a system consisting of (1-Me-Ind)Ni(PPh_3)Cl/$NaBPh_4$ can catalyze the addition of $PhSiH_3$ to styrene to give PhCH(Me)($SiPhH_2$) in up to 80 catalytic turnovers.[3] We have proposed that the mechanism of this reaction involves the insertion of styrene into the Ni−H bond of an intermediate to give a new Ni−alkyl species; the latter then reacts with a second $PhSiH_3$ to liberate the hydrosilylation product and regenerate the Ni−H intermediate. The initial Ni−H species arises from a reaction between the in-situ-formed Ni-based cations and $PhSiH_3$ (hydride abstraction); alternatively, it can be generated by reacting the Ni−X precursors with $LiAlH_4$ (X = Cl) or directly with $PhSiH_3$ (X = Me; Scheme 5). It should be noted, however, that the IndNi(PPh_3)Cl/$NaBPh_4$ combinations give faster rates and higher yields.[3]

(25) Previous observations on the analogous reactions of ethylene or 1-hexene with Ind−Ni-based systems have shown that these eliminations can be facile: Wang, R.; Groux, L. F.; Zargarian, D. *Organometallics* **2002**, *21*, 5531.

Table 4. Catalytic Formation of PhCH($PhSiH_2$)CH_3[a]

run	catalyst	time (h)	yield (%)
1	**1a**/$NaBPh_4$	24	70
2a	**1b**/$NaBPh_4$	6	70
b		24	74
3a	**1b**	6	<5
b		24	63
c		72	75
4a	**2b**	6	85
b		24	85
5	Ni(PPh_3)$_3$Cl	24	10
6	**3a**	24	80
7	[(1-Me-Ind)-Ni(PPh_3)$_2$][BPh_4][b]	24	5
8	**2b**[c]	24	50
9	**2b**[d]	24	93
10	**2b**[e]	24	52

[a] Unless otherwise specified, the reactions were run in C_6D_6 at room temperature using a Ni:$NaBPh_4$:styrene:$PhSiH_3$ ratio of 1:10:100:100. [b] Taken from ref 3. [c] 1000 equiv each of styrene and $PhSiH_3$ were used in this experiment. [d] A **2b**:styrene:$PhSiH_3$ ratio of 1:200:80 was used for this run. [e] A **2b**:styrene:$PhSiH_3$ ratio of 1:1500:1000 was used for this run.

In the present study, we selected styrene hydrosilylation as a test reaction for evaluating the catalytic activities of the complexes **1a**, **1b**, and **2b**.[23] Initial experiments were conducted under the same conditions as used in most of our previous studies, namely, room-temperature reactions employing a 1:10:100:100 ratio of Ni:$NaBPh_4$ (when needed):$PhSiH_3$:styrene and run over 6−24 h. The catalytic activity of unactivated **1b** was also examined briefly, because a recent study has shown that some Ni−Cl precursors can promote the hydrosilylation of styrene in the absence of $NaBPh_4$.[26] It should be noted that all of these reactions gave the same product, namely, PhCH($SiPhH_2$)Me, with virtually none of the other regioisomer, $PhCH_2CH_2(SiPhH_2)$, being detected by NMR. The quantitative results of the catalytic runs are listed in Table 4 and described below.

Runs 1−4 showed that hydrosilylation reactions catalyzed by **2b** give higher yields than those by **1a** or **1b**. The superior activity of **2b** was especially evident when shorter reaction times were employed or when the neutral precursors were used in the absence of the cationic initiator $NaBPh_4$. This point is better illustrated from the plots of yield vs time obtained by monitoring the progress of the catalysis promoted by **1b** and **2b** (Figure 6). As can be seen, the catalytic activity of **2b** requires little or no induction period and reaches a plateau 2−3 h after the start.

The reactivities of the Ni(I) species (PPh_3)$_3$NiCl and the bis(phosphine) species **3a** were also probed briefly. The Ni(I) species was found to be a poor precatalyst for the hydrosilylation reaction (Table 4, run 5), which implies that even if this side-product were present in solutions of **1a**, its contribution to the overall catalytic

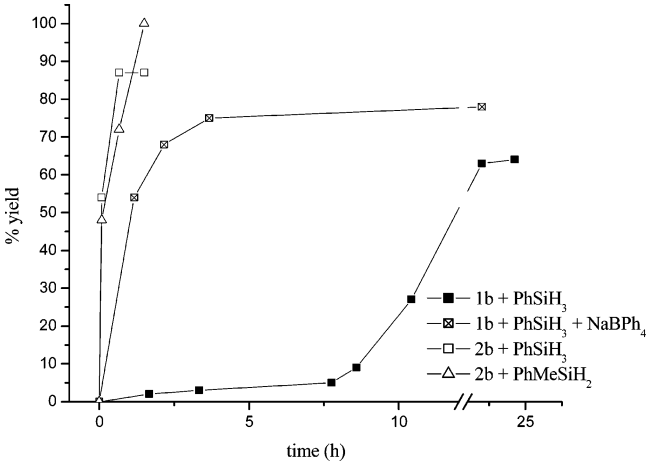

Figure 6. Kinetic profiles for the addition of $PhSiH_3$ or $PhMeSiH_2$ to styrene catalyzed by complex **1b** or **2b**. The experiments were carried out in C_6D_6 using a 1:(10:)50:50 ratio of precatalyst:($NaBPh_4$:)styrene:silane.

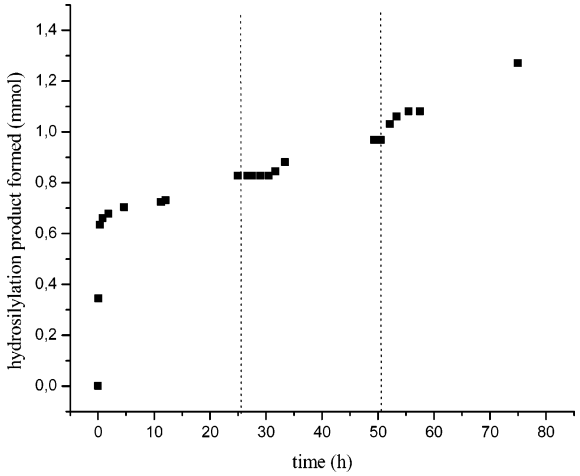

Figure 7. Kinetic plot of the addition of $PhSiH_3$ to styrene catalyzed by **2b**. New batches of substrates (50 equiv each) were added to the reaction mixture at the time intervals indicated by the dashed vertical lines.

activities would be insignificant. On the other hand, complex **3a** was found to be nearly as active as **2b** for promoting the addition of $PhSiH_3$ to styrene (compare runs 6 and 4b). Significantly, this level of activity is much higher than that of $[(1\text{-Me-Ind})Ni(PPh_3)_2]^+$ (run 7) and implies that the catalysis proceeds more efficiently in the presence of the pendant olefin moiety. Since the presence of a second PPh_3 ligand in the coordination sphere of Ni would be expected to hinder the approach of the much more weakly nucleophilic substrates, we propose that the higher reactivity of **3a** is due to the intramolecular displacement of the second PPh_3 ligand by the pendant olefin moiety. In other words, under the conditions of the catalysis, **3a** is effectively converted to a catalytically active species, probably via the intermediary of **2a** (eq 2).

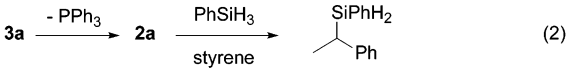

(2)

Optimizing the Catalytic Efficiency of 2b. To determine the highest level of hydrosilylation activity that can be obtained from **2b**, we conducted a number of experiments using smaller catalyst loadings, which showed that increasing the catalyst:substrate ratio leads to lower relative yields. For example, a 0.1% Ni loading gave only ca. 50% yield (run 8); although this corresponds to a higher number of catalytic turnovers in comparison to the runs using 1% loadings (ca. 500 vs 75−85), the diminishing relative yields imply that a deactivation takes place beyond the initial stages of the catalysis. To confirm this, we conducted an experiment in which additional batches of substrates were added to the reaction mixture after an interval of ca. 24 h and the reaction progress was monitored continuously. The results are plotted in Figure 7, which shows that the catalysis becomes increasingly sluggish after the initial phase. The extent of decline in the catalytic efficacy of **2b** is more clearly evident when we compare turnover frequency numbers at various stages during the three-day reaction period: 1.4 mmol/h during $t = 0-5$ h; 0.034 mmol/h during $t = 5-25$ h; 0.005 mmol/h during $t = 25-52$ h; 0.008 mmol/h during $t = 52-80$ h.[27]

The sharp decline in the catalytic activity of **2b** is presumably caused by a deactivation process that depletes the active species available for the hydrosilylation catalysis. We suspected that the most likely deactivation pathway involves possible side-reactions between $PhSiH_3$ and **2b** (or derivatives arising from it during the catalysis). To confirm this, we monitored the $^{31}P\{^1H\}$ NMR spectrum of a mixture of **2b** (ca. 0.02 M in C_6D_6) and $PhSiH_3$ (10 equiv) in the absence of styrene, which showed that the signal due to **2b** disappeared completely within 5 min of the mixing time and was replaced by several new ^{31}P resonances in the 40−43 ppm range. We have not isolated any of these new species, but their chemical shifts are in the range associated with complexes of the type (R-Ind)Ni(PPh_3)X (X = H and $SiPh_nH_{3-n}$ moieties).[28] On the other hand, monitoring the ^1H NMR spectra of the reaction mixture indicated that some or all of these new species continue reacting with $PhSiH_3$. These observations are consistent with the possibility that $PhSiH_3$ undergoes competitive side-reactions with **2b** and derivatives arising from it during the catalysis, thereby reducing the number of catalytically active species available for hydrosilylation.[29] It is reasonable to propose that such side-reactions would be more competitive when the concentration of styrene is depleted (toward the later stages

(26) Chen, Y.; Sui-Seng, C.; Boucher, S.; Zargarian, D. *Organometallics* **2005**, *24*, 149.

(27) Careful inspection of Figure 7 seems to indicate an upswing in the pace of catalysis toward the end of the 3-day period, presumably because of the accumulation of unreacted substrates in the reaction medium. This result should be treated with caution, however, given the relatively large uncertainties associated with the NMR integration values.

(28) The Ni−H derivatives are not stable enough to be isolated, but signals detected in the range 41−44 ppm during the decomposition of some bulky Ni−alkyl derivatives (alkyl = *t*-Bu, *i*-Bu, *sec*-Bu) have been attributed to them (refs 9 and 12). On the other hand, the $^{31}P\{^1H\}$ NMR (C_6D_6) spectrum of $IndNi(PPh_3)SiCl_3$ shows a singlet resonance at 49 ppm: Boucher, S.; Zargarian, D. Unpublished results.

(29) On the basis of previous studies, we believe that the most likely side-reaction is the dehydrogenative coupling of $PhSiH_3$ to give $(PhSiH)_n$ oligomers, but the ^1H NMR spectra recorded for the **2b**/$PhSiH_3$ mixtures do not show the characteristically broad signals associated with these materials. Other possibilities include insertion of the pendant olefin into a Ni−H bond or reductive elimination of R−Ind−H to from Ni(0) species. Or see: (a) Fontaine, F.-G.; Zargarian, D. *Organometallics* **2002**, *21*, 401. (b) Fontaine, F.-G.; Kadkhodazadeh, T.; Zargarian, D. *Chem. Commun.* **1998**, 1253.

of the hydrosilylatoin catalysis) or when a greater [**2b**]:[$PhSiH_3$] ratio is used. To examine the validity of this proposal, we carried out the following experiments.

First, we conducted catalytic reactions using an excess of styrene to determine if this would improve the reaction yields. Thus, a reaction using a 1:200:80 ratio of **2b**:styrene:$PhSiH_3$ gave an improved hydrosilylation yield of 93% (run 9), implying that the extent of unproductive side-reactions can be minimized in the presence of excess styrene. On the other hand, a similar reaction using a 1:1500:1000 ratio gave only 52% yield (run 10), which is not a significant improvement over the 1:1000:1000 reaction (run 8), implying that the greater silane concentration in large-scale runs counteracts the beneficial effects of excess styrene.

Next, we set out to determine if using secondary hydrosilanes instead of $PhSiH_3$ would affect the extent of unproductive side-reactions; since these silanes are less reactive than $PhSiH_3$ in dehydrocoupling reactions, they were expected to favor the hydrosilylation catalysis.[30] Indeed, the addition of $PhMeSiH_2$ or Ph_2SiH_2 to styrene was found to be nearly quantitative in less than 3 h, both in small-scale (1:100:100 ratio) and large-scale (1:1000:1000 ratio) reactions (Figure 6).[31] That the large-scale hydrosilylation of styrene proceeds more efficiently with a secondary silane such as $PhMeSiH_2$ (up to 1000 catalytic turnovers) than $PhSiH_3$ (up to 500 catalytic turnovers) is consistent with the proposal that the hydrosilylation is inhibited by unproductive side-reactions involving $PhSiH_3$.

Conclusion

The present study has shown that incorporating a pendant olefin moiety in Ind−Ni complexes renders the otherwise electronically and coordinatively unsaturated cations $[IndNi(PPh_3)]^+$ stable enough to be isolated and characterized, while the hemilabile nature of the chelation preserves the reactivities of these species. The spectroscopic and solid-state characterization of **2** provides a better understanding of the Ni−Ind and Ni−olefin interactions in such species. We have learned, for instance, that the unsymmetrical binding of the olefin might lead to the accumulation of positive charge on a vinylic carbon, thereby rendering the olefin susceptible to nucleophilic attacks; the facile polymerization of styrene in the presence of **2b** is consistent with this hypothesis. Thus, we believe that these complexes are good models for the proposed intermediates in Ni-catalyzed transformations of olefins. On the other hand, the labile binding of the pendant olefin in **2b** and **3a** facilitates the efficient hydrosilylation of styrene. On the basis of our experimental observations, we have proposed a few working hypotheses on how these catalytic reactions proceed and what type of deactivation pathways might be operating, but a detailed mechanistic picture will require further investigations.

(30) Tertiray hydrosilanes R_3SiH (R = Et, Ph, Cl) proved completely unreactive in our systems.

(31) It should be mentioned, however, that hydrosilylation of styrene with $PhMeSiH_2$ gives a 90:10 mixture of the regioisomers PhCH(SiPhMeH)CH_3 and $PhCH_2CH_2$(SiPhMeH), whereas the corresponding reaction with Ph_2SiH_2 gives only $PhCH_2CH_2(Ph_2SiH)$. In other words, the regioselectivity of the hydrosilylation depends on the nature of R in $PhRSiH_2$.

Experimental Section

General Comments. All experiments were conducted under an atmosphere of nitrogen using standard Schlenk techniques and/or a glovebox. Dry, oxygen-free solvents were used throughout. The elemental analyses were performed by Laboratoire D'analyse Élémentaire (Université de Montréal). The NMR spectra were recorded at ambient temperature on an AMX400 spectrometer. The GC/MS analyses were made on an Agilent Technologies 6890 Network GC system equipped with an HP-5MS capillary column and a 5973 MS selective detector. Synthetic procedures for the two indenyl ligands, 1-{CH_2=$CH(CH_2)_2$}-indene and 1-{CH_2=$CH(CH_2)SiMe_2$}-indene, have been reported previously.[6]

(η^3:η^0-Ind$(CH_2)_2$CH=CH_2)Ni(PPh_3)Cl (1a). An Et_2O solution (50 mL) containing Ind$(CH_2)_2CH$=CH_2 (0.270 g, 1.53 mmol) and *n*-BuLi (0.67 mL of a 2.5 M solution in hexane, 1.68 mmol) was stirred overnight and then transferred (dropwise over 3 h) to a stirred solution of $(PPh_3)_2NiCl_2$ (1.20 g, 1.83 mmol) in Et_2O (25 mL). After filtration and concentration, the product was precipitated with hexane. Washing the filtrate with cold hexane (2 × 20 mL, 0 °C) gave 0.168 g of red solid (21%). Single crystals suitable for X-ray analysis were obtained by slow diffusion of hexane into a saturated Et_2O solution. ^{1}H NMR (C_6D_6): δ 7.81 (m, PPh_3), 7.55 (m, H7), 7.27 (t, $^3J_{H-H}$ = 7.5, H6), 7.01 (t, $^3J_{H-H}$ = 7.4, H5), 6.57 (d, $^3J_{H-H}$ = 1.9, H2), 6.29 (d, $^3J_{H-H}$ = 7.4, H4), 6.11 (m, H10), 5.30 (d, $^3J_{H-H}$ = 16.9, H11A), 5.17 (d, $^3J_{H-H}$ = 10.0, H11B), 3.56 (s, H3), 2.80, 2.70, 2.47, and 2.20 (m, H8A, H8B, and H9A, H9B). ^{13}C{^{1}H} NMR (C_6D_6): δ 139.3 (C10), 135.1 (d, $^2J_{P-C}$ = 11.8, *o*-C), 133.2 (d, $^1J_{P-C}$ = 43.7, *i*-C), 130.9 (*p*-C), 130.4 (C7a), 129.1 (*m*-C), 127.4 (C3a), 127.1 and 126.8 (C5 and C6), 119.2 and 117.5 (C4 and C7), 115.7 (C11), 107.2 (d, $^2J_{P-C}$ = 13.2, C1), 103.4 (C2), 67.4 (C3), 31.7 and 26.9 (C8 and C9). ^{31}P{^{1}H} NMR (C_6D_6): δ 30.7. Anal. Calcd for $C_{31}H_{28}ClNiP$: C, 70.83; H, 5.37. Found: C, 70.61; H, 5.57.

(η^3:η^0-IndSi$(Me)_2CH_2CH$=CH_2)Ni(PPh_3)Cl (1b). An Et_2O solution (200 mL) containing IndSi$(Me)_2CH_2CH$=CH_2 (1.05 g, 4.9 mmol) and *n*-BuLi (2.00 mL of a 2.5 M solution in hexane, 5.0 mmol) was stirred overnight and then transferred (dropwise over 3 h) to a stirred solution of $(PPh_3)_2NiCl_2$ (3.5 g, 5.4 mmol) in Et_2O (25 mL). After filtration and concentration, the product was precipitated with hexane and washed with cold hexane (0 °C, 2 × 20 mL) to give 1.87 g of red solid (67%). Single crystals suitable for X-ray analysis were obtained by slow diffusion of hexane into a saturated Et_2O solution. ^{1}H NMR (C_6D_6): δ 7.94−7.81 (m, PPh_3), 7.68 (d, $^3J_{H-H}$ = 8.1, H7), 7.30 (t, $^3J_{H-H}$ = 7.3, H6), 7.04 (t, $^3J_{H-H}$ = 7.5, H5), 6.78 (d, $^3J_{H-H}$ = 2.5, H2), 6.52 (d, $^3J_{H-H}$ = 7.6, H4), 6.13 (m, H10), 5.20 (d, $^3J_{H-H}$ = 17.0, H11A), 5.13 (d, $^3J_{H-H}$ = 9.1, H11B), 3.65 (d, $^3J_{H-H}$ = 3.1, H3), 2.28−2.15 (m, H9A & H9B), 0.83 (s, Si-*Me*), 0.81 (s, Si-*Me*). ^{13}C{^{1}H} NMR (C_6D_6): δ 135.4 (C10), 134.5 (d, $^2J_{P-C}$ = 11.1, *o*-C), 134.3 (C7a), 132.3 (d, $^1J_{P-C}$ = 43.7, *i*-C), 130.5 (*p*-C), 129.5 (C3a), 128.5 (d, $^3J_{P-C}$ = 10.3, *m*-C), 127.1 and 126.0 (C5 and C6), 121.5 and 117.6 (C4 and C7), 113.6 (C11), 109.7 (C2), 93.6 (d, $^2J_{P-C}$ = 13.9, C1), 72.9 (C3), 24.4 (C9), −2.70 and −2.93 (C8A and C8B). ^{31}P{^{1}H} NMR (C_6D_6): δ 28.58. Anal. Calcd for $C_{32}H_{32}ClNiPSi$: C, 67.45; H, 5.66. Found: C, 67.79; H, 5.56.

[(η^3:η^2-Ind$(CH_2)_2CH$=CH_2)Ni(PPh_3)][BPh_4] (2a). A CH_2Cl_2 solution of **1a** (70 mg, 0.13 mmol) and $NaBPh_4$ (320 mg, 0.93 mmol) was stirred for 2 h at room temperature and then filtered. The product was precipitated with Et_2O to give a brown-red solid (41 mg, 45%). Microcrystals were obtained by repeated recrystallization from CH_2Cl_2/Et_2O. ^{1}H NMR ($CDCl_3$): δ 7.69 (d, $^3J_{H-H}$ = 7.1, H7), 7.60−7.01 (m, PPh_3, H2, H5, and H6), 6.52 (d, $^3J_{H-H}$ = 7.1, H4), 5.63 (s, H3), 5.48 (m, H10), 4.05 (d, $^3J_{H-H}$ = 16.1, H11A), 3.09 (t, $^3J_{H-H}$ = 7.1, 11B), 2.54 and 2.05 (m, H8A, H8B and H9A, H9B). ^{13}C{^{1}H} NMR ($CDCl_3$): δ 133.3 (d, $^2J_{P-C}$ = 11.1, *o*-C), 131.8 (*p*-C), 129.5 (d, $^3J_{P-C}$ = 13.2, *m*-C), 128.3 (d, $^1J_{P-C}$ = 46.5, *i*-C),

120.3 (C4), 119.5 (C7), 114.7 (d, $^2J_{P-C}$ = 10.4, C1), 112.3 (C10), 105.5 (C2), 92.2 (C3), 71.8 (C11), 36.5 and 21.9 (C8 and C9). $^{31}P\{^1H\}$ NMR ($CDCl_3$): δ 33.66. Anal. Calcd for $C_{31}H_{30}BF_4NiP \cdot H_2O$: C, 62.57; H, 5.08. Found: C, 62.41; H, 5.10.

[(η^3:η^2-IndSi(Me)$_2$allyl)Ni(PPh$_3$)][BF$_4$] (2b). A CH_2Cl_2 solution of **1** (300 mg, 0.53 mmol) and $AgBF_4$ (113 mg, 0.58 mmol) was stirred for 1 h at room temperature in an ultrasonic bath and then filtered. The product was precipitated and washed with hexane to give a brown solid (165 mg, 46%). ^1H NMR ($CDCl_3$): δ 7.52−7.20 (m, PPh_3, H7, H6, H5, and H2), 6.56 (d, $^3J_{H-H}$ = 7.6, H4), 5.48 (s, H3), 5.40 (m, H10), 3.90 (d, $^3J_{H-H}$ = 16.2, H11A), 3.18 (t, $^3J_{H-H}$ = 7.1, H11B), 2.52 (dd, $^2J_{H-H}$ = 6.9, $^3J_{H-H}$ = 12.1, H9A or H9B), 1.86 (dd, $^2J_{H-H}$ = 4.5, $^3J_{H-H}$ = 12.5 H9A or H9B), 0.70 (s, Si-*Me*), 0.60 (s, Si-*Me*). $^{13}C\{^1H\}$ NMR (CD_2Cl_2): δ 133.3 (d, $^2J_{P-C}$ = 10.7, *o*-C), 132.1 (*p*-C), 131.0 and 129.8 (C5 and C6), 129.5 (d, $^2J_{P-C}$ = 10.7, *m*-C), 127.8 (d, $^1J_{P-C}$ = 47.0, *i*-C), 126.9 (C7a), 122.1 (C3a), 121.4 and 121.3 (C4 and C7), 110.5 and 110.0 (C10 and C2), 104.5 (d, $^2J_{P-C}$ = 8.8, C1), 91.6 (C3), 75.0 (C11), 26.3 (C9), −0.18 and −2.68 (C8A and C8B). $^{31}P\{^1H\}$ NMR ($CDCl_3$): δ 33.70. Anal. Calcd for $C_{32}H_{32}ClNiPSiBF_4$: C, 61.88; H, 5.19. Found: C, 60.84; H, 5.04.

[(η^3:η^0-Ind(CH$_2$)$_2$CH=CH$_2$)Ni(PPh$_3$)$_2$][BPh$_4$] (3a). Multiple recrystallization of **2a** in hot CH_2Cl_2/hexane gave **3a** as a yellow solid. ^1H NMR (CD_2Cl_2): δ 7.50−6.91 (m, PPh_3, BPh_4, H5 and H6), 6.56 (d, $^3J_{P-H}$ = 2.0, H2), 6.30 (d, $^3J_{H-H}$ = 6.9, H4 or H7), 6.05 (d, $^3J_{H-H}$ = 7.0, H4 or H7), 5.55 (m, H10), 4.98 (d, $^3J_{P-H}$ = 2.4, H3), 4.86 (d, $^3J_{H-H}$ = 10.1, H11B), 4.75 (d, $^3J_{H-H}$ = 17.1, H11A), 2.15−2.00 (m, H9A and H9B), 1.48 and 1.26 (m, H8A and H8B). $^{13}C\{^1H\}$ NMR (CD_2Cl_2): δ 163.9 (4-line multiplet, $^1J_{B-C}$ = 49, *i*-C of BPh_4), 136.5 (C10), 136.0 (*m*-C of BPh_4), 133.7 (d, $^2J_{P-C}$ = 10.9, *o*-C of $Ph_3P(1)$), 133.5 (d, $^2J_{P-C}$ = 11.2, *o*-C of $Ph_3P(2)$), 131.3 and 130.7 (*p*-C of both PPh_3), 130.3 (d, $^1J_{P-C}$ = 46.6, *i*-PPh_3), 129.1 to 128.3 (*m*-C of both PPh_3, C5 and C6), 125.6 (d, $^3J_{P-C}$ = 2.3, *o*-C of BPh_4), 124.2 and 122.8 (C3a and C7a), 121.7 (*p*-C of BPh_4), 119.6 and 119.4 (C4 and C7), 115.8 (C11), 105.8 (d, $^2J_{P-C}$ = 10.1, C1), 104.3 (C2), 83.1 (d, $^2J_{P-C}$ = 9.2, C3), 32.5 (d, $^3J_{P-C}$ = 4.5, C8), 25.83 (C9). $^{31}P\{^1H\}$ NMR (CD_2Cl_2): δ 35.4 and 32.2 (d, $^2J_{P-P}$ = 26.7). Anal. Calcd for $C_{73}H_{63}BNiP_2$: C, 81.81; H, 5.93. Found: C, 80.56; H, 5.78.

[(η^3-allyl)Ni(PPh$_3$)$_2$][BF$_4$] (4). Recrystallization of **2b** in CH_2Cl_2/Et_2O gave brown crystals, which were identified as the known complex **4**[20] on the basis of the NMR spectra and microanalysis. ^1H NMR (C_6D_6): δ 7.30 (m, PPh_3), 5.75 (m, H2), 3.83 (m, H syn or anti), 3.17 (m, H syn or anti). $^{31}P\{^1H\}$ NMR (C_6D_6): δ 26.66. Anal. Calcd for $C_{39}H_{35}BF_4NiP_2$: C, 65.87; H, 4.96. Found: C, 65.64; H, 5.02.

General Procedure for Carrying Out Catalytic Polymerization of Styrene. Polymerization reactions were carried out by stirring a mixture of **2b** (ca. 10 mg, 0.0175 mmol) and a large excess of styrene for a given length of time, as follows. Run 1 was carried out in dichloroethane (8 mL) using ca. 2000 equiv of styrene; the mixture was stirred at 60 °C for 48 h. Runs 2−5 were carried out in toluene (1 mL) or neat styrene (ca. 1000 equiv); the mixtures were stirred for 4 h at 60 or 25 °C (see Table 3). The final reaction mixtures obtained from runs 1, 4, and 5 were evaporated to remove the solvent and/or unreacted styrene, followed by dissolving the solid residues in a minimum of toluene and transferring into ethanol to precipitate an off-white solid. The reaction mixtures in runs 2 and 3 solidified in 3−4 h; workup of these mixtures consisted of dissolving the solid residues in a minimum of toluene and transferring into ethanol to precipitate an off-white solid. The solid products were subjected to NMR and GPC analyses; the latter were done using THF as solvent and were calibrated on the basis of poly(styrene) standards.

General Procedure for Conducting Catalytic Hydrosilylation of Styrene. Most runs were carried out in NMR tubes containing C_6D_6 (ca. 0.8 mL), **2b** (ca. 10 mg, 0.0175 mmol), styrene (ca. 200 μL, 1.76 mmol), and $PhSiH_3$ (ca. 210 μL, 1.76 mmol); $NaBPh_4$ (ca. 55 mg, 0.17 mmol) was also added to the reaction mixture in some runs (see Table 4). The tubes were placed in an ultrasonic bath at room temperature for the desired period of time. NMR spectroscopy allowed us to identify the reaction product by comparison to authentic samples, which were obtained from large-scale runs, distilled, and fully characterized by NMR and GC/MS. The yields were determined from the relative integration values for the substrate and product protons, on the basis of a calibration curve prepared as described previously.[26] The kinetic runs were conducted similarly, but using 50 equiv of substrates.

Acknowledgment. The authors gratefully acknowledge the financial support provided by NSERC of Canada and useful discussions with Sylvain Boucher and Michel Simard.

Supporting Information Available: Complete details on the X-ray analyses of **1a**, **1b**, **2a**, **3a**, and **4**, including tables of crystal data, collection, and refinement parameters, bond distances and angles, anisotropic thermal parameters, and hydrogen atom. This material is available free of charge via the Internet at http://pubs.acs.org.

OM050285U